Optimization of the key parameters in the carrot seed guiding system using DEM-CFD analysis

Yue Sun[1], Lianglong Zhang[1,2], Fan Yang[1], Fangyan Wang[1*], Jingtao Jiang[2]

(1. *College of Mechanical and Electrical Engineering, Qingdao Agricultural University, Qingdao 266109, China*;
2. *Collaborative Innovation Center for Shandong Main Crop Production Equipment and Mechanization, Qingdao 266109, China*)

Abstract: The objective of this research was to enhance the stability and consistency of seed distribution during carrot planting. The impact of the seed guide tube's structure on seeding quality was examined, leading to the design of a cycloidal seed guide system augmented by positive pressure airflow. By conducting kinematic modeling of the collision position of the seeds within the seed guiding system, as well as considering the seed guiding process and the seed drop position, the significant parameters influencing the final velocity of the seeds were determined. Employing a coupled Discrete Element Method-Computational Fluid Dynamics (DEM-CFD) simulation, the effects of different structural and operating parameters of the seed guide tube on the seed trajectory and airflow field were analyzed. A three-factor five-level orthogonal test was then utilized to examine the influence of each factor on each index, with the optimal conditions identified as an inlet airflow velocity of 0.077 m/s, a 45° tilt angle for the airflow branch tube, and a seed initial velocity of 0.1 m/s. Under these parameters, the qualification index was recorded as 94.1%, with a coefficient of variation of 3.2%. Bench testing conducted under the same conditions showed a decrease of 0.07% in the qualification index, and an increase of 1.875% in the coefficient of variation, with errors relative to the simulation results within acceptable bounds. These findings enhance the stability and reliability of the seed guiding system during carrot sowing operations, aligning with the demands of precision sowing.

Keywords: carrot, seed guiding process, seed motion analysis, air assisted, DEM-CFD
DOI: 10.25165/j.ijabe.20251806.9763

Citation: Sun Y, Zhang L L, Yang F, Wang F Y, Jiang J T. Optimization of the key parameters in the carrot seed guiding system using DEM-CFD analysis. Int J Agric & Biol Eng, 2025; 18(6): 112–121.

1 Introduction

With the advancements in mechanized seeding technology in China, the cultivation of carrots has seen a shift towards mechanized single-grain seeding operations, with the air suction carrot seeder serving as the primary model. The core of mechanized seeding is precision sowing and orderly seed movement. This apparatus is capable of efficiently performing seed suction, transportation, cleaning, and discharge. The technical specifications for achieving precise single-seed rows have been fulfilled. However, the seed guide system presents a challenge, as seeds often collide with the variable trajectory seed guide tube, resulting in inconsistent seed spacing and compromising the overall seeding quality of the air-suction carrot seeder[1-5].

Currently, research on seed guiding technology for carrots is extremely limited, with primary focus on crops featuring larger seed sizes, such as corn and soybeans. The seed tube integrated with the Horsch MAESTRO SW pneumatic precision planter[6] features a cross-section that tapers from a wider top to a narrower bottom, enhancing seed guiding stability for corn[7]. Maschio Gaspardo's CHRONO high-speed planter employs an airflow-driven seed delivery method, where seeds wrapped in an air stream slide rapidly down the tube before being projected into the soil[8]. However, neither of these machine types meets the requirements for single-seed sowing of carrots. Kuhn's[9] Maxima series air-assisted seeders utilized a centralized distributor for pneumatic seed transport, yet achieving precise control over seed movement trajectory and airflow velocity within the tube remains challenging[10].

The positive-pressure airflow-assisted seed guiding system employs air thrust to accelerate seeds, thereby reducing their chaotic collisions with the tube walls during the guiding process, ensuring smooth and synchronized seed placement into the soil. Due to the complexity and challenges involved in analyzing seed motion and flow fields during the guiding process, a particle-fluid coupling simulation method is crucial for optimizing and analyzing the positive-pressure airflow-assisted seed guiding device.

Seed delivery systems assisted by positive-pressure airflow utilize the thrust of the air stream to accelerate seeds. This reduces disordered collisions with the tube wall during seed conveyance, enabling stable seed delivery with uniform time intervals between seeds. Analyzing the motion of seeds and the airflow field during the delivery process is highly demanding and challenging. Consequently, a coupled simulation approach for particles and fluid is required to optimize the design of the seed delivery device.

Shi et al.[11] employed DEM-CFD coupled analysis to optimize the structure of the seed metering device, thereby improving seed pickup performance for maize. Ding et al.[12] utilized gas-solid coupling simulation to model the working process of a pneumatic seed metering device, obtaining the sequence of pickup capability for different seed types. Wang[13] took typical small-seeded crops such as rape, sesame, and pakchoi as examples and analyzed the

Received date: 2025-03-03 **Accepted date:** 2025-08-12
Biographies: Yue Sun, MS candidate, research interest: agricultural machinery and equipment, Email: sunyue_2808@163.com; **Lianglong Zhang**, MS, candidate, research interest: agricultural machinery and equipment, Email: 20222104035@stu.qau.edu.cn; **Fan Yang**, PhD, Lecturer, research interest: agricultural engineering, Email: yf1762773980@163.com; **Jingtao Jiang**, PhD, Lecturer, research interest: design and development of modern agricultural equipment, Email: jjtao_2518@163.com.
***Corresponding author: Fangyan Wang**, PhD, Professor, research interest: design and theory of agricultural equipment. College of Mechanical and Electrical Engineering, Qingdao Agricultural University, Qingdao 266109, Shandong, China. Tel: +86-15806426016, Email: wfy_66@163.com.

kinematics and dynamics models of key processes in air-assisted seed delivery and seed placement using DEM-CFD coupled simulation. However, the influence of the airflow field on seed movement trajectory was not investigated in depth. Zhang et al.[14] from Qingdao Agricultural University employed EDEM software to design the seed delivery path for carrots, developing a seed tube curve equation based on a quadratic function. This improved the qualified seeding rate, but achieving zero-speed seeding remained unrealized.

To address the issue of low seed velocity and difficulty matching machine forward speed in seed delivery systems designed based on the principle of cycloidal isochronicity[15], this study developed a positive-pressure air-assisted cycloidal seed delivery system. This system utilizes the entrainment effect of the airflow to reduce collisions between seeds and the inner wall of the delivery tube. While accelerating the seeds, it simultaneously constrains them to slide down along the tube wall, ensuring the cycloidal isochronicity condition is maintained. This achieves the dual mechanisms of "isochronous seed delivery" and "gentle seed conveyance". By establishing kinematic models for seeds at different stages of the delivery path, the key parameters influencing zero-speed seeding accuracy were derived. Based on Discrete Element Method-Computational Fluid Dynamics (DEM-CFD) coupled simulation technology, the influence patterns of these key parameters on seed trajectory, airflow field distribution, and transport time were analyzed. The structural and operational parameters of the delivery system were optimized using the orthogonal experimental design method. The validity of the optimized solution was then verified through bench tests. This research aims to provide theoretical support for improving the zero-speed seeding accuracy and stability of carrot seed delivery systems.

2 Materials and methods

2.1 Structure and principle of air-aspirated seed guiding system

The carrot air suction seed guide system comprises an air suction seed discharger, seed guide tube, and a positive pressure airflow auxiliary device, as illustrated in Figure 1. Under negative pressure, the seeds are adsorbed on the discharge disk and rotate with it, thereby entering the seed casting area where they come into contact with the seed guide member, the direction of motion changes, and subsequently travel down the seed guide tube. Within the seed guide tube, an amalgamation of seeds and positive pressure airflow occurs, compelling the seeds to be coerced along the seed guide tube wall before sliding into the seed groove to complete the seeding process. It is important to note that during the descending process, heightened friction and collision between the seed and the seed guide tube can lead to instability in seed transport[16]. Consequently, the seed guide system is the key component to ensure the isochronous seed transportation and smooth seed drop, and its structure directly affects the seeding quality. According to the carrot seed casting trajectory to optimize the structure of the seed guide system, the airflow conveying pipe is designed according to the shape of the grafting port of the tree branch, and the airflow is a uniform turbulent state in the seed guide pipe, so that the seeds enter the seed guide pipe and interact with it to form a uniform two-phase flow of gas and solid. The wrapping of the airflow restricts the freedom of the seeds, reduces the disordered collision with the seed guide tube while accelerating the seeds, makes the transportation time of neighboring seeds more uniform, and improves the sowing quality.

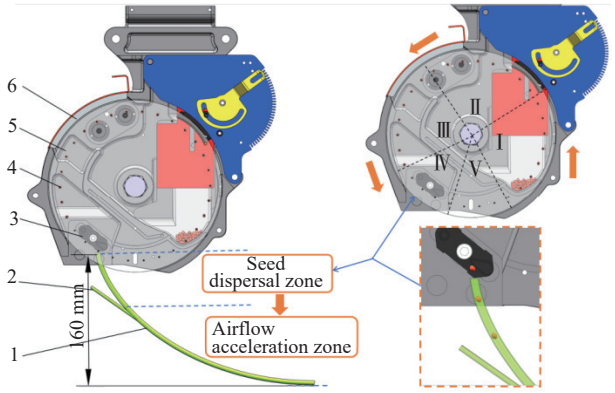

1.Positive pressure airflow-assisted seed guide device 2.Airflow inlet 3.Seed guide 4.Seed 5.Row of seed discs 6.Air suction seed discharger; Ⅰ. The various areas within the device are labeled as the suction seed area; Ⅱ. Seed clearing area; Ⅲ. Seed carrying area; Ⅳ. Seed casting area; Ⅴ. Blowing miscellaneous area.

Figure 1 Structure of the seed guiding device of the air-absorbent seed discharger

2.2 Analysis of the movement of carrot seeds in the seed guide tube

2.2.1 Analysis of the seed motion at collision position

The seed is discharged from the seed discharger and subsequently enters the seed guide tube at a velocity denoted as U_0. Upon entry, the first collision between the seed and the wall of the seed guide tube occurs. This collision results in a modification of both the magnitude and direction of the seed's velocity. Specifically, the velocity of the seed prior to the collision, denoted as U_0, and the collision recovery coefficient between the seed and the material of the seed guide tube, assumed to be a constant value, collectively determine the motion characteristics and velocity of the seed post-collision, as dictated by the reflection angle β_2. The velocity analysis of the seed at the collision position is shown in Figure 2.

$$\begin{cases} v_n = eu_0 \sin\beta_2 \\ v_t = u_0\left[\mu\sin\beta_2(e-1)+\cos\beta_2\right] \\ v_0 = \sqrt{v_n^2+v_t^2} \end{cases} \tag{1}$$

where, e is the coefficient of recovery of collision between carrot coated seeds and ABS material.

2.2.2 Analysis of the motion of the seed at acceleration process

In order to ensure the isochronous nature of the seeds in the seed guide process and to reduce the sowing time[17], the pendulum seed guide tube equation is incorporated into the seed guide tube equation, and the pendulum equation is:

$$\begin{cases} x = a(\theta+\sin\theta) \\ y = a(1-\cos\theta) \end{cases} \tag{2}$$

where, a is the radius of the moving circle, m; θ is the angle at which the fixed point on the moving circle is turned, (°).

The seed enters the seed guide tube and slides along the inner wall of the tube under the action of positive pressure airflow, and the mechanical model of the sliding process is as follows:

$$\begin{cases} F_N - mg\cos\varphi = ma_n \\ R + mg\sin\varphi - F_f = ma_\tau \\ a_n = \dfrac{v^2}{\rho} \\ a_\tau = \dfrac{\mathrm{d}v}{\mathrm{d}t} \\ F_f = \mu F_N \end{cases} \tag{3}$$

where, a_n is the centripetal acceleration to which the seed is subjected, m/s²; a_τ is the tangential acceleration to which the seed is subjected, m/s²; F_f is the sliding friction force on the seed, N; ρ is the radius of curvature of the pendulum, m; μ is the coefficient of friction between the seed and the wall of the tube.

The distance of the seed from the collision position to the airflow acceleration area is short, and the resistance of the air to the seed can be neglected in this process, so the only resistance to the seed during airflow acceleration is friction:

$$F_f = \mu\left(mg\cos\varphi + m\frac{v^2}{\rho}\right) \tag{4}$$

In order to simplify the analysis of the seed acceleration process in the airflow, the carrot-coated seeds were analyzed by looking at them as spheres; the airflow thrust on a single seed moving in the airflow is R[18].

$$R = \frac{2}{3}g\rho_s d_s\frac{V_a - V}{V_b}\pi r^2 \tag{5}$$

where, ρ_s is the particle density, kg/m³; d_s is the particle radius, m; V_a is the airflow velocity, m/s; V_b is the suspension velocity of carrot-coated seeds, m/s; V is the end velocity of seeds after airflow acceleration, m/s; r is the radius of seed guide tube, m.

The airflow branch of the positive pressure airflow assist device intersects tangentially with the left and right walls of the seed guide tube. The specific location of the tangent point serves to dictate both the angle of inclination between the airflow branch and the seed guide tube, and the airflow conditions present at the interface. In accordance with Figure 2, the position of the gas transmission pipeline may be subject to further adjustments through the modification of the tilt angle, denoted as α. The determination of the range for α, specifically within 25°-55°, is guided by the constraints imposed by pipeline tangency and mating positions.

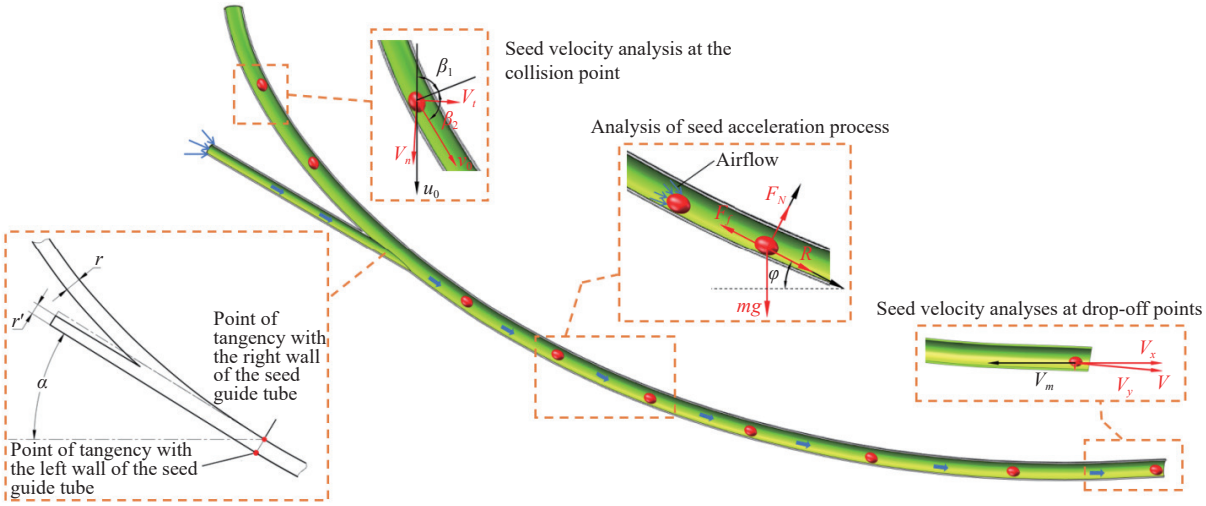

Note: β_1 denotes the angle of incidence in degrees, (°); β_2 indicates the angle of reflection in degrees, (°); U_0 represents the pre-collision velocity, m/s; V_0 is the post-collision velocity, m/s; V_n is the post-collision normal velocity, m/s; V_t is the post-collision tangential velocity, m/s; F_N is the support force on the seed of the wall of the tube, N; F_f is the sliding friction force, N; R is the airflow thrust, N; mg is the gravitational force of the seed, N; φ is the inclination angle of the seed tube, (°); V is the terminal velocity of the seed leaving the seed guide tube, m/s; V_x is the terminal velocity horizontal velocity, m/s; V_y is the terminal velocity vertical velocity, m/s; V_m is the forward speed of the machine, m/s; r' is the radius of the airflow branch pipe, m; α is the angle at which the airflow branch is tangent to the seed guide tube, (°).

Figure 2 Motion analysis of seeds in the seed guiding process

The magnitude of the airflow, denoted as V_a, exerts a notable influence on the air thrust exerted on the seeds within the tube. It is imperative that the airflow creates a stable laminar flow upon entry into the seed guide tube. Throughout the process of seed guidance, the airflow must be calibrated to facilitate seed acceleration without causing their dispersion. Compliance with the prerequisites for the establishment of laminar flow[19], as well as the stipulated criteria governing airflow magnitude during seed guidance, is imperative.

$$\begin{cases} R_e = \dfrac{2\rho_s V_a r}{\eta} < 2320 \\ \mathrm{mg} + R\sin(90^\circ - \varphi) \geq F_N\sin\varphi \end{cases} \tag{6}$$

where, R_e is the Reynolds number; and η is the aerodynamic viscosity coefficient, Pa·s.

Getting the airflow delivered in the seed guide tube V_a, the range is:

$$0 < V_a < \frac{2.35}{r^2} \tag{7}$$

Given the positioning of the airflow inlet at the positive pressure airflow assist device's inlet, we can leverage Bernoulli's equation to ascertain the inlet airflow at the airflow branch tube by assessing the ratio between the radius of the seed guide tube and the radius of the branch tube. Denoted as V_a, this represents the airflow size at the branch pipe[20]. k is introduced to represent the ratio between the radius of the airflow branch pipe r' and the radius of the seed guide pipe r, $k = \dfrac{r'}{r}$. The value of k falls within the range of 0-1.

2.2.3 Analysis of the motion of the seed at drop point

According to the kinetic energy theorem during seed introduction:

$$\frac{1}{2}mV^2 - \frac{1}{2}mV_0^2 = mgh + RS - F_f S \tag{8}$$

The equation for the velocity V at the end of the seed leaving the outlet of the seed guide tube is obtained:

$$\left(\frac{1}{2}m + \frac{\mu S m}{\rho}\right)V^2 + \frac{g\rho_s d_s\pi r^2 S}{3V_b}V - \frac{1}{2}mV_0^2 - mgh - \frac{2}{3}g\rho_s d_s\pi r^2 S\frac{V_a}{V_b} + \mu\mathrm{mg}\cos\varphi = 0 \tag{9}$$

where, S is the arc length of the seed guide tube, m[21].

After the seed reaches the drop point with velocity V, in order to reach the zero-speed casting[22], the following requirements need to be satisfied:

$$V_x = V\cos\varphi = V_m \tag{10}$$

Upon determining the spatial arrangement and material composition of the seed guide tube and the seed guide system, a range of parameters come into play. These include the reflection angle β_2, the arc length S of the seed guide tube, the radius of curvature ρ, the radius r of the seed guide tube, the tilt angle φ of the seed guide tube, the levitation speed of the seed V_b, the mass of a single seed m, the diameter d_s of the seed, the flow density ρ_s of the seed, the collision recovery coefficient between the seed and the material of the seed guide system, the friction coefficient μ, the Reynolds number R_e, and the aerodynamic viscosity coefficient η. The initial velocity V_0 of the seed entering the seed guide tube, the inlet airflow velocity V_a, the pipe diameter ratio k, and the angle of inclination of the input airflow pipe α are also influential factors that impact the velocity of the seeds as they pass through the seed guide system.

2.3 Simulation analysis of seed guide tube

The airflow field inside the seed guide tube affects the acceleration effect of seeds, which in turn affects the sowing quality. In order to study the influence of the airflow field on the acceleration effect of seeds, the airflow field inside the seed guide tube was analyzed by single-factor and orthogonal tests using DEM-CFD coupled simulation[23], and the pressure distribution and velocity distribution inside the tube were analyzed with different structural and operating parameters, with the aim of obtaining the optimal sowing quality of the seed guide tube. The purpose was to obtain the seed guide tube with optimal seeding quality under different structural and working parameters. The velocity of seeds in the seed guiding process and the seed guiding time between neighboring seeds were obtained by EDEM post-processing to obtain the effect of collision on seed guiding time and to verify the isochronous nature of seed guiding[24].

2.3.1 Model and simulation parameterization

(1) Seed guide tube meshing

The seed guide tube model is imported into ANSYS Workbench, the internal cavity of the tube is set as the fluid domain, the airflow inlet and outlet are set, mesh delineation is carried out, and the part of the interface between the airflow delivery tube and the seed guide tube is encrypted, and the mesh quality meets the simulation requirements[25].

(2) DEM-CFD simulation parameterization

In order to conduct soil simulation effectively and efficiently, a soil slot of dimensions 1000 mm×500 mm×80 mm was established using EDEM software. After investigating the soil composition of Shandong Province, it was determined that the soil for carrots planting is loose and has good flow properties[26]. For the simulation, the Hertz-Mindlin (no slip) contact model was selected to represent the interactions between soil particles[27]. To meet the requirements for planting carrots, trenchers were used to excavate the soil slot to a depth of 20 mm, creating the seed furrow. In Fluent software, the fluid medium was defined as air, the airflow inlet was selected as the inlet of the airflow conveying tube, and the standard k-ε model was chosen for the transient calculation of the turbulence model. The tube wall was defined with a no-slip wall condition, and the standard wall function was employed. The pressure-based SIMPLE (Semi-Implicit Method for Pressure-Linked Equations) algorithm was selected for the coupled solution. To ensure simulation stability, the coupled simulation was initiated only after the Fluent simulation had reached a steady state[28]. The residual convergence criteria for the Fluent simulation were set as follows: residuals for all variables, except energy, were required to fall below 10^{-3}, while the convergence criterion for the energy residual was set below 10^{-6}[29]. Therefore, whether model convergence was achieved could be reliably determined based on the stabilization observed in the residual convergence curve plots. The parameters used for the coupled simulation are summarized in Table 1.

Table 1 Coupling simulation parameters

	Parameters	Value		Parameters	Value
Gas	Gravitational acceleration/m·s^{-2}	9.81	Carrot-coated seeds	Poisson's ratio	0.2
	Density/kg·m^{-3}	1.225		Density/kg·m^{-3}	1130
	Stickiness/kg·m^{-1}·s^{-1}	1.789×10^{-5}		Shear modulus/Pa	6×10^{6}
Seed guide	Poisson's ratio	0.39	Seed guide with carrot-coated seeds	Coefficient of restitution	0.55
	Density/kg·m^{-3}	1060		Coefficient of static friction	0.45
	Shear modulus/Pa	8.96×10^{8}		Coefficient of rolling friction	0.06

Various iterations of the seed guide system were simulated using 3D software, with different modifications made to the inclination angles and tube diameter ratios. The resulting models were saved in.stl format and subsequently imported into EDEM software (see Figure 3).

In order to accurately quantify the uniformity and stability of the designed seed-guiding components, we have chosen the qualified index (y_1) and coefficient of variation (y_2) as the test parameters. These selections are in accordance with the standards GB/T 6973-2005 Test Methods for Single Grain (Precision) Seeders and JB/T 10293-2001 Technical Conditions for Single Grain (Precision) Seeders. The coefficient of variation serves as the metric for assessing the stability of seed guiding, while the qualified index is utilized to evaluate the overall uniformity of the seed discharger and seed-guiding components. These indices collectively provide a comprehensive means of assessing the performance of the seed-discharging and guiding mechanisms.

$$\begin{cases} y_1 = \dfrac{n_0}{N} \times 100\% \\ y_2 = \sqrt{\dfrac{\sum (X - \bar{X})^2}{(n' - 1)\bar{X}^2}} \times 100\% \end{cases} \tag{11}$$

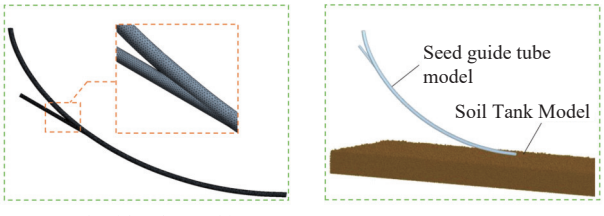

a. Seed guide tube meshing b. Seeding simulation

Figure 3 Simulation model

where, y_1 is the qualified index, %; y_2 is the coefficient of variation, %; n_0 is the number of single seed rows, pcs; N is the theoretical number of seed rows; n' is the total number of sample hole spacing; X is the theoretical sowing hole spacing, cm; $\bar{x}$ is the average value of sample hole spacing, cm.

Three sets of replicated trials were conducted to investigate the distances between neighboring seeds using the Ruler tool for post-processing in EDEM software. These distances were measured, incorporated into a formula, and then calculated to determine the eligibility index and coefficient of variation.

2.3.2 Simulation test content and method

(1) Single factor test

To validate the soundness of the theoretical analysis and examine the impact of the seed guide system's structure on the airflow field and seed movement characteristics, simulation studies were conducted. These studies assessed the effects of the inlet airflow velocity V_a', the radius ratio (k) between the radius of the seed guide tube and the radius of the airflow branch tube, the tilt angle (α) of the input airflow tube, and the initial velocity (V_0) on the gas-solid two-phase flow. The initial velocity V_0 of the seeds into the seed guide tube was taken as five factors, 0.05 m/s, 0.1 m/s, 0.15 m/s, 0.2 m/s, 0.25 m/s; the inlet gas velocity was taken as four factors, 0.04 m/s, 0.06 m/s, 0.08 m/s, 0.1 m/s; the tube diameter ratio k was taken as three factors, 1/2, 1/3, 2/3; and the angle of inclination of the inlet gas tube was taken as six factors, 25°, 30°, 35°, 40°, 45°, 50°, to conduct a one-factor simulation test to analyze the effects of different factors on the gas pressure and velocity inside the seed guide tube and the seeds inside the tube. Six factors were taken as 25°, 30°, 35°, 40°, 45°, 50°, and a one-factor simulation test was carried out to analyze the effects of the different factors of the test on the pressure and velocity of the gas in the seed-guide pipe and the velocity of the seeds in the seed-guide pipe.

(2) Orthogonal tests

A three-factor, five-level orthogonal test was carried out on the basis of the one-factor test, and the factor coding table is shown in Table 2. A coupled simulation method was used to accurately simulate the movement process of carrot-coated seeds in the seed guide tube. The test factors were the initial velocity V_0 of the seeds entering the seed guide tube, the inlet airflow velocity V_a', and the tilt angle of the input airflow pipelineα. The test indices were the qualification index y_1 and the coefficient of variation y_2. The goal was to analyze the effects of different indices on the seed guide time and the number of collisions of the seeds, and to get the optimal structural parameters of the seed guide tube and the optimal combination of seed guide. The best combination of structural parameters of the seed guide tube and the best combination of working parameters of the seed guide are obtained.

Table 2 Factor coding table

Encodings	Inlet air velocity V_a'/m·s^{-1}	Tilt angle α/(°)	Initial velocity V_0/m·s^{-1}
1.682	0.046	30	0.016
–1	0.06	35	0.05
0	0.08	42.5	0.1
1	0.1	50	0.15
1.682	0.114	55	0.184

2.4 Bench testing

In order to validate the accuracy of the simulation test, the experimentation was conducted on the JPS-12 Seed Displacement Performance Testing Test Bench at Qingdao Agricultural University, depicted in Figure 4. The engineered seed guiding system was manufactured and affixed to the air suction seed discharger employing 3D printing technology[30]. The input airflow speed was set at 0.077 m/s, with the airflow pipe inclined at 45°, and the initial seed velocity at 0.1 m/s. The velocity of the seed bed belt was set to 0.24 m/s, corresponding to the actual forward speed of the seeder. Subsequent to sowing, the seeds were sampled and the interplant spacing among 50 seeds was measured. The sampling process was repeated thrice and the resultant data averaged to compute the qualification rate and coefficient of variation.

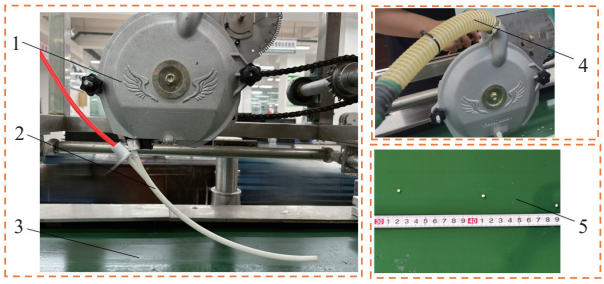

1.Air suction seed discharger 2.Positive pressure airflow assisted seed guide device 3.Seed bed belt 4.Negative pressure airflow pipe 5.Sowing effect picture

Figure 4 Bench test and seeding effect

3 Results and analysis

3.1 Analysis of the results of the one-way test

3.1.1 Impact of pipe diameter ratio on airflow field and seed velocity

Figure 5 illustrates the influence of different diameter ratios on the airflow velocity field, static pressure field, and seed velocity within the seed delivery tube. Analysis reveals the following:

At a diameter ratio of 1/3: A stable acceleration zone forms at the connection point. However, the overall airflow velocity within the tube is the lowest, and the static pressure approaches ambient pressure, resulting in minimal acceleration of the seeds. A significant velocity gradient exists between the connection point and the upper region, subjecting seeds to substantial airflow impact. The seed velocity trajectory plot indicates a high collision frequency, adversely affecting the seed descent velocity and delivery time.

At a diameter ratio of 1/2: The airflow velocity contour plot shows airflow primarily concentrated in the upper section of the delivery tube, with lower velocities in the delivery zone. The static pressure contour plot similarly indicates insufficient dynamic pressure in the delivery zone. Seeds entering the delivery zone lack effective airflow encapsulation. The seed velocity trajectory plot displays non-smooth velocity curves within the delivery zone, also leading to unstable velocity and prolonged delivery time.

At a diameter ratio of 2/3: Airflow velocity profile stratification is observed at the tube inlet, but the overall velocity is low. Seed inflow velocity is uniform, indicating the stratification does not adversely affect the initial seed motion. The velocity gradient at the connection point is small, resulting in minimal impact on seeds during entry. Within the delivery zone, airflow velocity is stable, and static pressure distribution is uniform, ensuring seeds receive consistent acceleration and effective encapsulation throughout the descent. The corresponding seed velocity trajectory is smooth, exhibiting no significant rebound behavior. This effectively ensures the realization of "isochronous seed delivery" and "gentle seed conveyance".

Based on the analysis of the aforementioned flow field characteristics and seed motion stability, the seed delivery tube with

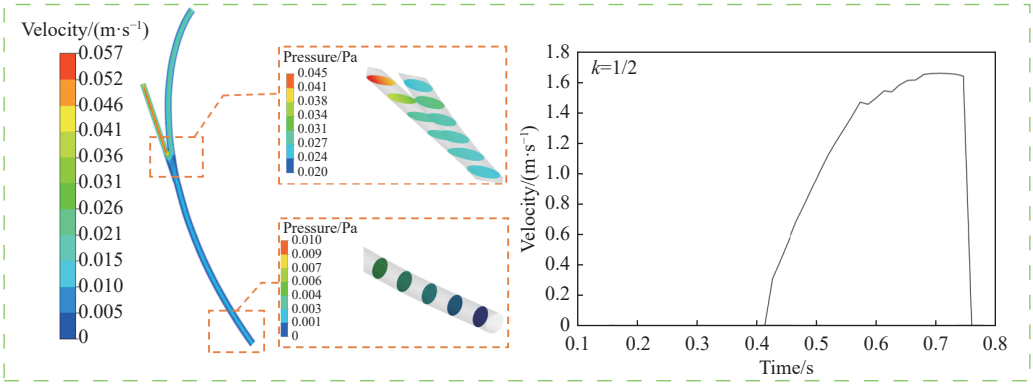

a. Seed guide tube velocity cloud

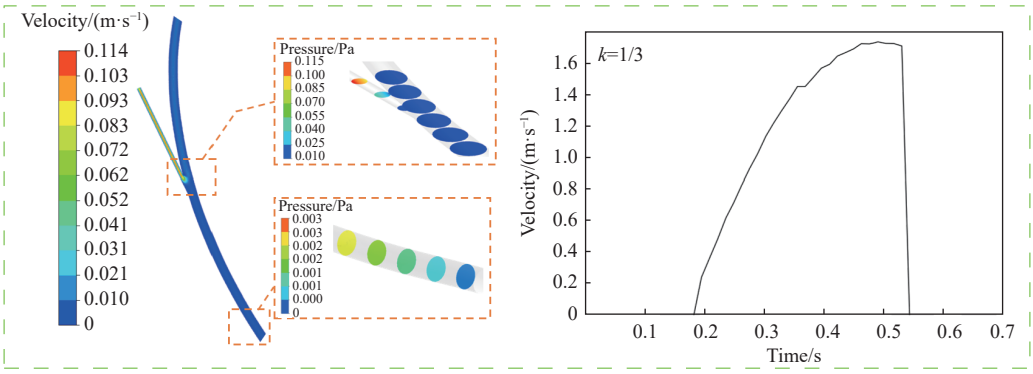

b. Airflow pressure cloud map

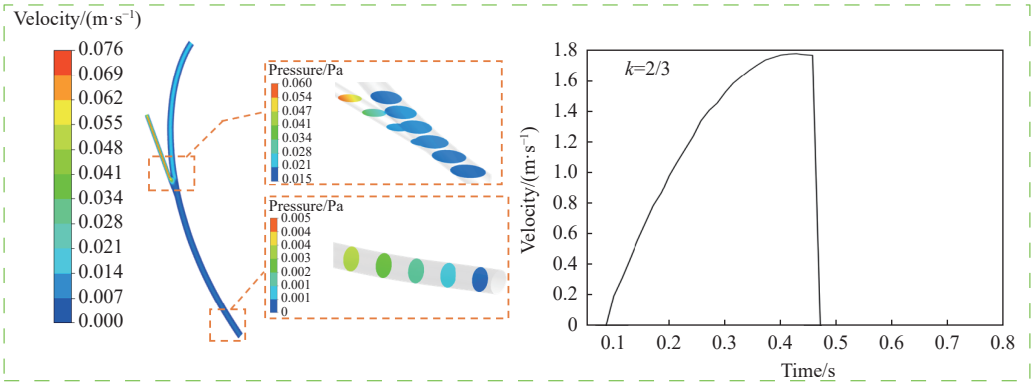

c. Seed velocity map

Figure 5 Effect of pipe diameter ratio on airflow field and seed velocity

a diameter ratio of 2/3 was selected for subsequent testing.

3.1.2 Impact of conveyor pipe inclination angle on airflow field

As shown in Figure 6, the tilt angle of the conveying pipe affects the relative position of the airflow branch pipe and the seed guide tube. When α=25°, the airflow branch pipe and the seed guide pipe angle is too small to make the airflow into the seed guide pipe on the direct and the pipe right wall surface impact. From Figure 6a of the trace diagram, it can also be known that the exit direction at this time of most of the airflow through the articulation to the seed guide pipe. The seeds fall from the inlet after the impact of the airflow is larger, making the seed velocity in the process of seed guiding unstable, bouncing more times; see Figure 6g. With the increase of the tilt angle of the conveying pipe, the positive pressure airflow from the pipe into the guide tube gradually guides the seed tube seed inlet direction, to guide the seed tube outlet out of the airflow is reduced and articulation of the airflow pressure decreases, the airflow density decreases. The seed movement velocity curve gradually smooths, with less bouncing phenomenon, when α=45° and 50°, where the velocity curve is smooth and the seed shows almost no bouncing. When α=30°-50°, the airflow distribution at the interface of the two tubes is uniform and there is no vortex area or stagnation area, and the gas mixing in the seed guide tube is uniform.

3.1.3 Impact of inlet air velocity on seed trajectories

The effect of the inlet air velocity on the movement of seeds is shown in Figure 7. When the air velocity is 0.04 m/s and 0.06 m/s, the airflow and the seed is difficult to mix to become a uniform two-phase flow, so the acceleration of the airflow on the seed under this condition is small, as shown in Figure 7b. The seed in the falling process and the seed guide tube wall collision times, as shown in Figure 7a. When the inlet air velocity increases to 0.08 m/s and 0.10 m/s, the seed and airflow mix into a uniform two-phase flow, the seed in the airflow under the package speed increases, the number of collisions is less, and the trajectory tends to be smooth.

3.1.4 Impact of initial velocity on seed trajectory

As shown in Figure 8, when the seed with an initial velocity of 0.05-0.1 m/s is falling, in the positive pressure airflow and the seed package uniformity, so that the seed in the process of guiding the

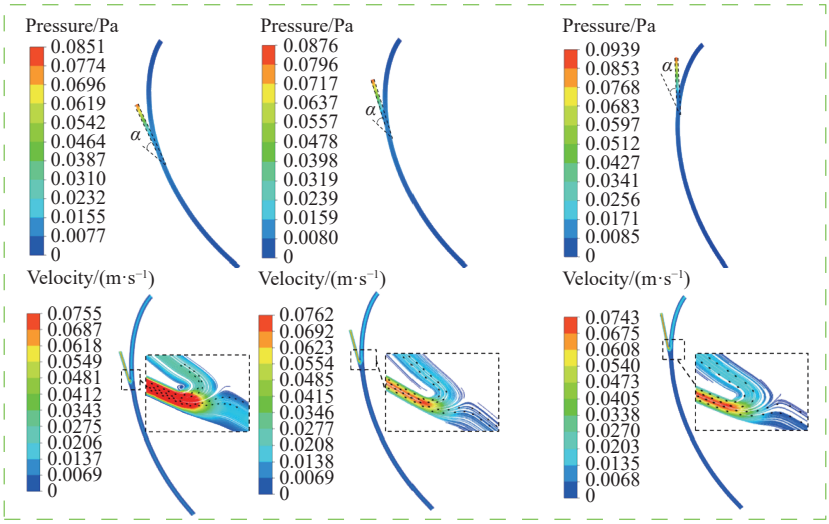

a. α=25°

b. α=30°

c. α=35°

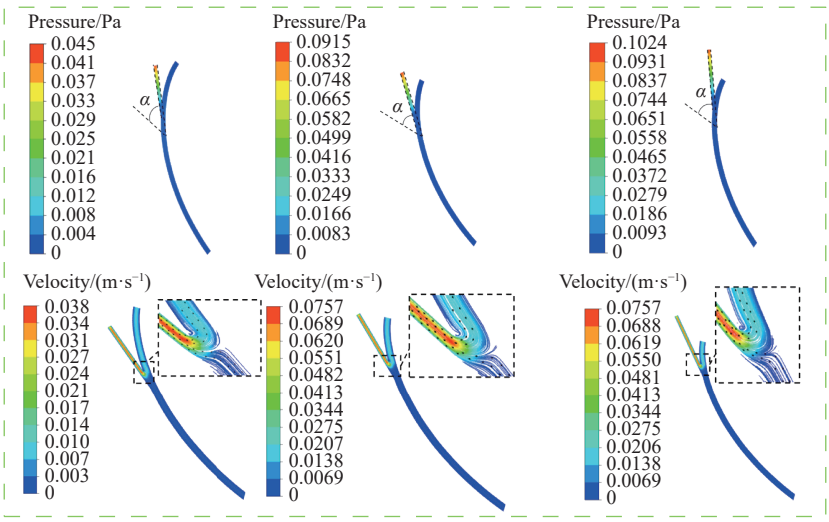

d. α=40°

e.α=45°

f. α=50°

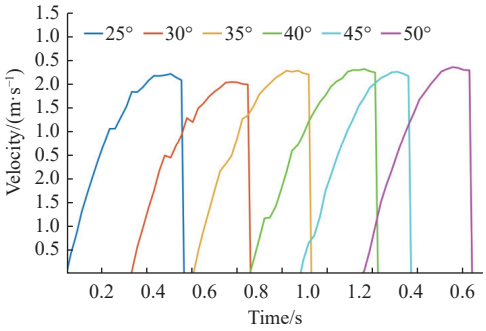

g. Seed velocity graphs at different tilt angles

Figure 6 Effect of inclination angle of conveyor pipe on airflow field and seed velocity

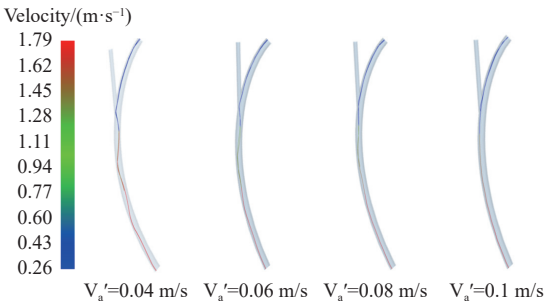

a. Effects on seed trajectories

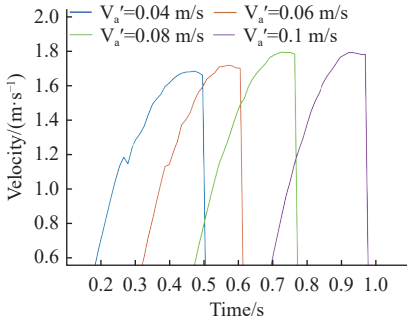

b. Effect on the rate of seed conductivity

Figure 7 Influence of conveyor air velocity on seed trajectory and seed guiding velocity

seed slides along the wall of the tube, the velocity curve is smooth and with almost no bounce. At this time, the seed by the wall of the tube friction force is less, and the total force is small. The initial velocity is 0.15 m/s when the seed begins to appear bouncing, and more turning points appear in the velocity curve. With the initial velocity increased to 0.2-0.25 m/s, the airflow and the degree of wrapping of the seed is lower and lower, so that the seed in the falling process experienced an increase in the number of bounces. From the left side of Figure 8 in the velocity trajectory diagram, it can also be known that, at this time, the seed's descent speed also increased. Therefore, the lack of airflow on the seed package, the seed in the process of falling with the seed guide tube wall of the contact more, by the force is large.

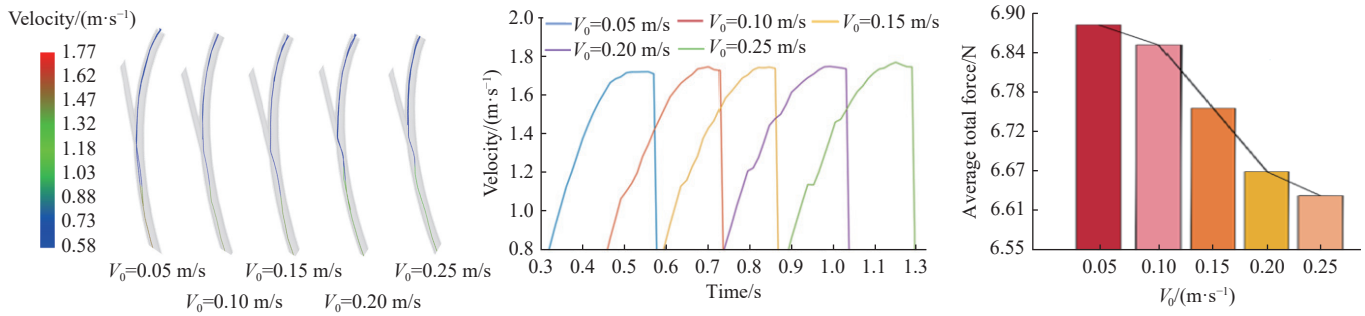

Figure 8 Effect of seed initial velocity on seed guiding trajectory, velocity and forces

3.2 Analysis of orthogonal test results

Considering the outcomes of the simulation test along with the agronomic requirements for carrot sowing, experimental factors including seed guide tube radius (r=3), ratio of guide tube length to diameter (k=2/3), inlet air velocity (V_a'=0.06-0.1 m/s), tilt angle (α 35°-50°), and initial velocity (V_0=0.05-0.15 m/s) were selected. These selections provide a solid theoretical foundation for subsequent parameter optimization tests.

Using coated carrot seeds as the subject of investigation, the test parameters included inlet airflow speed, tilt angle, and initial velocity, while the assessment criteria comprised of qualification index and coefficient of variation. With the help of Design-Expert software, a three-factor five-level orthogonal test was designed. Regression analysis of the test results screened out the significant factors and obtained the regression equations affecting the qualification index and coefficient of variation[2].

$$y_1 = 91.84 + 4.69x_1 + 3.77x_2 - 2.83x3 - 3.84x_1^2 - 2.52x_2^2 - 3.38x_3^2 + 2.99x_1x_2 \quad (12)$$

$$y_2 = 6.22 - 4.75x_1 - 3.45x_2 + 3.26x_3 + 1.38x_1^2 + 1.51x_2^2 + 2.04x_3^2 - 2.19x_1x_3 \quad (13)$$

The effects of the factors on the seeding pass rate were in the following order: airflow speed>tilt angle>initial speed, and the interaction term between airflow speed and tilt angle had a significant effect on the pass rate. The effects of the factors on the coefficient of variation were in the following order: airflow velocity > tilt angle > initial velocity, and the interaction term between airflow velocity and initial velocity had a significant effect on the coefficient of variation. The effects of significant interaction terms on pass rate and coefficient of variation are shown in Figure 9.

As shown in Figure 9a, when the tilt angle is certain, with the increase of the input airflow speed, the uniformity of the gas-solid two-phase flow is improved. In addition, the airflow has good wrapping on the seeds, which restricts the freedom of movement of the seeds when they are leaving. The seed flow flows uniformly from the seed guide tube, the sowing uniformity is stabilized, and the sowing qualification rate is improved. When the input airflow is certain, the increase of tilt angle makes the airflow impact on the inner wall of the seed guide tube at the articulation smaller, which reduces the collision phenomenon caused by the airflow impingement after the seed enters, increases the uniformity of the seed guide, and increases the qualified rate. The coefficient of variation represents the uniformity of seeding spacing and also reflects the stability of seed guiding. As shown in Figure 9b, when the initial velocity of the seed is certain, the increase of the input air velocity makes the seed in the seed guide process improve the order of the seed, forming uniform seed flow into the seed trench and reducing the coefficient of variation of the sowing. When the input air velocity is certain, the increase of the initial velocity makes the

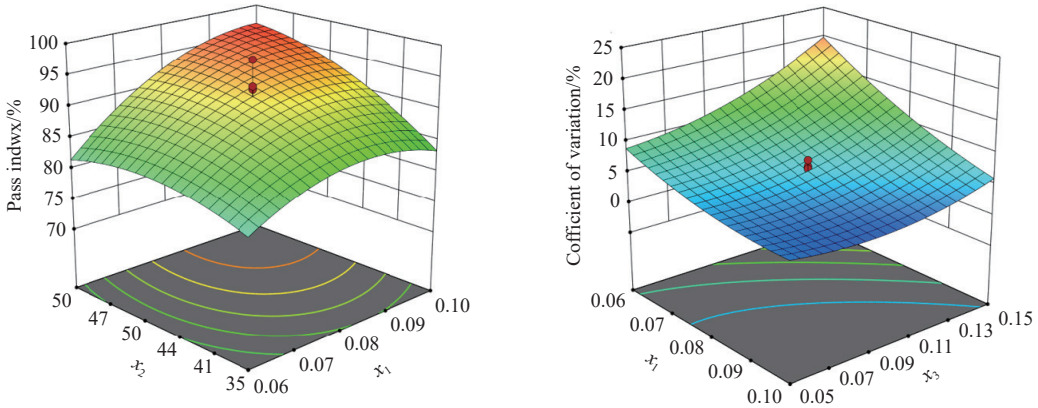

a. Effect of x_1x_2 interaction term on pass index

b. Effect of x_1x_3 interaction term on pass indexcoefficient of variation

Figure 9 Impact of interaction terms on indicators

seed in the exit of the seed guide tube go at a higher speed, and it is difficult to realize the zero-speed casting. When the seed is larger when landing, it is difficult to maintain the spacing of the grain, increasing the coefficient of variation.

Based on these considerations, the optimal combination of test factors was sought through the implementation of an optimal design and the establishment of a mathematical model. Regression equations for the qualification index and coefficient of variation were subsequently analyzed in conjunction with the boundary conditions of the test factors, ultimately leading to the derivation of a comprehensive mathematical model.

$$\begin{cases} \max y_1 \\ \min y_2 \\ \text{s.t.} \begin{cases} 0.046\ \text{m/s} \le V_a' \le 0.114\ \text{m/s} \\ 30^\circ \le \alpha \le 55^\circ \\ 0.0159\ \text{m/s} \le V_0 \le 0.0184\ \text{m/s} \\ 0 < y_1 \le 100 \\ 0 < y_2 \le 100 \end{cases} \end{cases} \quad (14)$$

Based on the multi-objective optimization module in the software to analyze and solve the mathematical model, with an inlet airflow speed of 0.077 m/s, tilt angle of 45°, and initial velocity of 0.1 m/s, the best uniformity of sowing and the stability of the seed guide is achieved. The best combination of parameters was used to carry out simulation experiments to verify the qualification index of 94.1% and the coefficient of variation of 3.2%. randomly selected six seeds to obtain The speed and time of seed guide were calculated to be 0.34 s, and the standard deviation was 0.0084 s, indicating that isochronous seed guide could be realized under the best parameter combination, as shown in Figure 10.

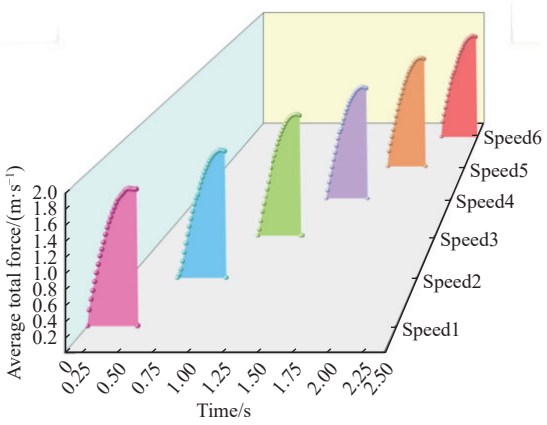

Figure 10 Time and speed of carrot seed guidance

3.3 Analysis of bench test results

As shown in Figure 11, the average qualification index in the actual test was 94.68%, and the coefficient of variation was 2.8%. Compared with the simulation test results, the qualification index was reduced by 0.07%, and the coefficient of variation was increased by 1.875%, which indicated that the designed positive-pressure airflow-assisted seed-guiding device had good seed-guiding stability and sowing uniformity, and the established CFD-DEM coupled simulation model could simulate the whole seed-guiding process more accurately.

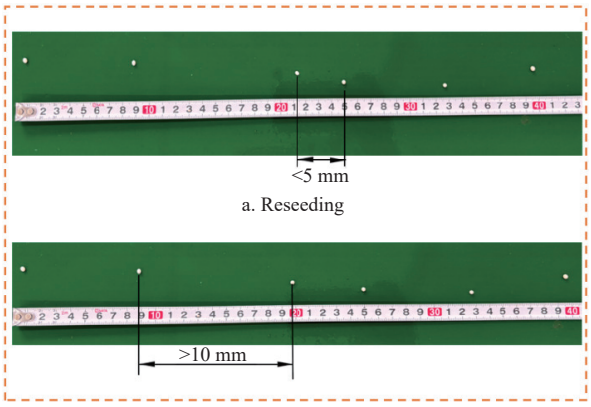

a. Reseeding

b. Miss seeding

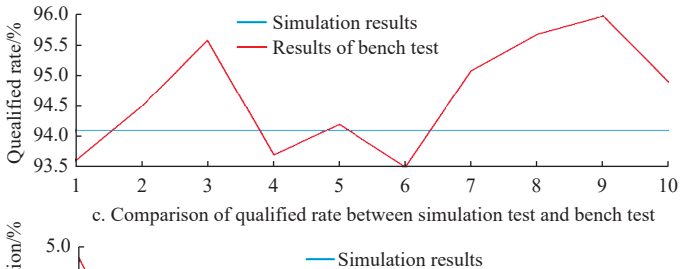

c. Comparison of qualified rate between simulation test and bench test

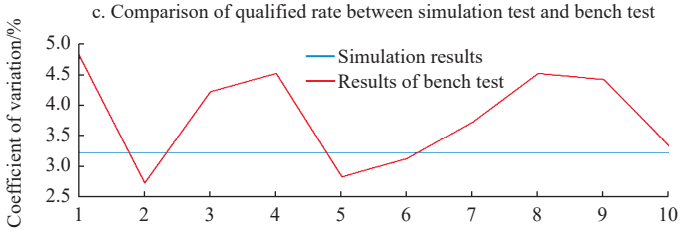

d. Comparisonofcoeffcientofvariation between simulationtestand bench test

Figure 11 Plot of bench test results

4 Conclusions

In this study, a positive-pressure airflow-assisted carrot seed guiding system was designed to utilize the flexible combination of airflow and carrot seeds to complete the seed guiding process. Through kinematic analysis of the seeds during the guiding process, we established a relationship between seed terminal velocity and the inlet airflow velocity, the inclination angle of the input airflow pipe, and the seed's initial velocity.

Leveraging the discrete element method, we developed a model for the interaction between the seed guide system and carrot-coated seeds. We simulated the seed motion within the guide system using a coupled DEM-CFD technique. Our simulations, analyzing the impact of the system's structure and working parameters on seed motion characteristics and airflow field, revealed that optimal mixing uniformity of the two-phase flow and seed velocity were achieved when the ratio of the radius of the seed-guiding tube to the radius of the airflow branch tube was 1/2. Furthermore, we observed that the end velocity of the seed increased with the inlet airflow velocity and the tilt angle of the airflow branch tube, while decreasing with the initial velocity. Additionally, we noted that the interface between the airflow branch tube and the seed guide tube exhibited no airflow vortex area or stagnation area, indicating that the seed slip power primarily originated from fluid thrust.

Employing Design-Expert software, we conducted a three-factor, five-level orthogonal test to establish an optimization model using multi-objective optimization methods. The inlet airflow velocity, the tilt angle of the input airflow pipe, and the initial seed velocity were designated as test factors, with qualification index and coefficient of variation as test indices. The results indicated that an

inlet airflow velocity of 0.077 m/s, a tilt angle of 45° for the airflow branch pipe, and an initial seed velocity of 0.1 m/s resulted in the best uniformity and stability of seed guiding, yielding a qualification index of 94.1% and a coefficient of variation of 3.2%.

Subsequent to bench experiments, we verified the simulation results, obtaining an average qualification index of 92.6% and a coefficient of variation of 6.1%, with small relative error compared to the simulation test results. These findings demonstrate the system's capability to meet the requirements of carrot seeding, significantly improving the stability of seed guiding and the uniformity of seed discharge.

Acknowledgements

This study was supported by the National Natural Science Foundation of China (Grant No. 52275258), Taishan Scholar Youth Expert Project (Grant No. tsqn202306243), and Natural Science Foundation of Shandong Province (Grant No. ZR202111230084).

[References]

[1] Zhang X, Wang L X, Zhou J H, Lian Y, Wang Y H, Chen C, et al. Cultivation technology of carrot in winter greenhouse in northern Jiangsu Province. Changjiang Vegetable, 2024; 13: 51–54. (in Chinese)

[2] Babojanov A B, Dulliev A K, Turdibekov A R. Development of a seeder design for precise sowing of carrot seeds on a ridge. IOP Conference Series: Earth and Environmental Science, IOP Publishing, 2022; 1076(1). DOI: 10.1088/1755-1315/1076/1/012071

[3] Wang F Y, Yang L, Wang H T. Design and test of electric driving pneumatic carrot planter in greenhouse. Transactions of the CSAM, 2022; 53(8): 64–73, 131. (in Chinese)

[4] Yan B X, Wu G W, Fu W Q, Gao N N, Meng Z J, Zhu P. Influencing factors of corn lm plantation distribution for high-height planting based on EDEM. Transactions of the CSAM, 2020; 51(S2): 47–54. (in Chinese)

[5] Huang X M, Zhang S, Zhu Y Z, Liu Y. Seeding process analysis and test of the air conveying rapeseed aerial seeding device. Transactions of the CSAE, 2022; 38(17): 31–41. (in Chinese)

[6] Zhang R. Study on precision depth-control mechanism of corn no-till planter in double-cropping area. China Agricultural University, 2016. (in Chinese)

[7] Chen Z J. Design and experiment on V-groove dialing round type seed-guiding device of maize precision planting machine. Northeast Agricultural University, 2019. (in Chinese)

[8] Yang L, Yan B X, Zhang D X, Zhang T L, Wang Y X, Cui T. Research progress on precision planting technology of maize. Transactions of the CSAM, 2016; 47(11): 38–48. (in Chinese)

[9] Yuan Y W, Bai H J, Fang X F, Wang D C, Zhou L M, Niu K. Research progress on maize seeding and its measurement and control technology. Transactions of the CSAM, 2018; 49(9): 1–18. (in Chinese)

[10] Chen Y L, jing H R, Zhang Z, Guo Y H, Ning X F. Design and experiment of the key components of the seedingmonomer for high-speed corn no-till seeders. Int J Agric & Biol Eng, 2023; 16(5): 95–103.

[11] Shi S, Liu H, Wei G J, Zhou J L, Jian S C, Zhang R F. Optimization and experiment of pneumatic seed metering device with guided assistant filling based on EDEM-CFD. Transactions of the CSAM, 2020; 51(5): 54–66. (in Chinese)

[12] Ding L, Yang L, Zhang D X, Cui T, Gao X J. Design and experiment of seed plate of corn air suction seed metering device based on DEM-CFD. Transactions of the CSAM, 2019; 50(5): 50–60. (in Chinese)

[13] Wang B S. Design and experiment of precision hill-seeding centralized metering system for small particle size seeds. Huazhong Agricultural University, 2023. (in Chinese)

[14] Wang F, Zhang W, Jiang J. Seed guide path planning and parameter optimization for air-suction carrot seed-metering device. Int J Agric & Biol Eng, 2023; 16(5): 104–112.

[15] Wang H J, Qian F. An eigenvalue method based on the steepest descent curve. Journal of Nantong University, Natural Science Edition, 2007; 1: 20–22. (in Chinese)

[16] Liao Y T, Li C L, Liao Q X, Wang L. Research progress of seed guiding technology and device of planter. Transactions of the CSAM, 2020; 51(12): 1–14. (in Chinese)

[17] Zhang X J, Chen Y, Shi Z L, Jin W, Zhang H T, Fu H, et al. Design and experiment of double-storage turntable cotton vertical disc hole seeding and metering device. Transactions of the CSAE, 2021; 37(19): 27–36. (in Chinese)

[18] Yan F, Cheng S, Rinoshika A, Song B, Jin G Q, Zhang J. Particle motion characteristics on the rotational flow pneumatic conveying of horizontal-vertical pipeline. Chemical Engineering Research and Design, 2024; 210: 452–468.

[19] Chen K W. Stability analysis of pipe flow and modeling of laminar-turbulent interface. Tianjin University, 2021. (in Chinese)

[20] Li Y J, Liu Y H, Liu L J. Distribution mechanism of airflow in seed tube of different lengths in pneumatic seeder. Transactions of the CSAM, 2020; 51(6): 55–64. (in Chinese)

[21] Liu X M, Deng J Y. Theoretical analysis of reasonable shape of seed guide tube for high speed precision seeder. Journal of Agricultural Mechanization Research, 1987; 4: 35–39. (in Chinese)

[22] Liu Q W. Design and experiment of seed precise delivery mechanism for high-speed planter. China Agricultural University, 2017. (in Chinese)

[23] Lei X L, Zhang W N, Li S S, Wang D, Liao Q X. Simulation and experiment of gas-solid flow in seed conveying tube for rapeseed and wheat. Transactions of the CSAM, 2017; 48(3): 57–68. (in Chinese)

[24] Liu W J, Shan Z, Chen X G. Design and experiment of spiral step cleaning device for ratooning rice based on CFD-DEM coupling. Computers and Electronics in Agriculture, 2024; 224: 109207.

[25] Li W X, Zhang F B, Luo Z T, Zheng E L, Pan D C, Qian J, et al. Straw movement and flow field in a crushing device based on CFD-DEM coupling with flexible hollow straw model. Biosystems Engineering, 2024; 242: 140–153.

[26] Zhang R, Han D X, Ji Q L, He Y, Li J Q. Calibration methods of sandy soil parameters in simulation of discrete element method. Transactions of the CSAM, 2017; 48(3): 49–56. (in Chinese)

[27] Wang X L, Zhong X K, Geng Y L, Wei Z C, Hu H, Geng D Y, et al. Struction and parameter calibration of the nonlinear elastoplastic discrete element model for no-tillage soil compaction. Transactions of the CSAE, 2021; 37(23): 100–107. (in Chinese)

[28] Xin N. Simulation analysis of working process of air-blowing seed-metering device based on coupled EDEM-FLUENT. Jilin University, 2013. (in Chinese)

[29] Xing H, Cao X M, Zhong P, Wan Y K, Lin J J, Zang Y, et al. DEM-CFD coupling simulation and optimisation of rice seed particles seeding a hill in double cavity pneumatic seed metering device. Computers and Electronics in Agriculture, 2024; 224: 109075.

[30] Liu L J, Yang H. 3D reverse engineering of seed guide tubes based on geomagic design software. Transactions of the CSAE, 2015; 31(11): 40–45. (in Chinese)